Supplementary information

Unravelling the room temperature growth of two-dimensional h-BN nanosheets for multifunctional applications

Abhijit Biswas,*[a,g] Rishi Maiti,[b,g] Frank Lee,[c,g] Cecilia Y. Chen,[d] Tao Li,[e] Anand B. Puthirath,[a] Sathvik Ajay Iyengar,[a] Chenxi Li,[a] Xiang Zhang,[a] Harikishan Kannan,[a] Tia Gray,[a] Md Abid Shahriar Rahman Saadi,[a] Jacob Elkins,[a] A. Glen Birdwell,[f] Mahesh R. Neupane,[f] Pankaj B. Shah,[f] Dmitry A. Ruzmetov,[f] Tony G. Ivanov,[f] Robert Vajtai,[a] Yuji Zhao,[e] Alexander L. Gaeta,*[b,d] Manoj Tripathi,*[c] Alan Dalton[c] and Pulickel M. Ajayan*[a]

[a] *Department of Materials Science and Nanoengineering, Rice University, Houston, Texas 77005, USA.*

[b] *Department of Applied Physics and Applied Mathematics, Columbia University, New York, 10027, USA.*

[c] *Department of Physics and Astronomy, University of Sussex, Brighton BN1 9RH, United Kingdom.*

[d] *Department of Electrical Engineering, Columbia University, New York, 10027, USA.*

[e] *Department of Electrical and Computer Engineering, Rice University, Houston, TX, 77005, USA.*

[f] *DEVCOM Army Research Laboratory, RF Devices and Circuits, Adelphi, Maryland 20783, USA.*

[g] *Abhijit Biswas, Rishi Maiti and Frank Lee equally contributed to this work*

[*] **Authors to whom correspondence should be addressed:** abhijit.biswas@rice.edu, m.tripathi@sussex.ac.uk, a.gaeta@columbia.edu, ajayan@rice.edu

Keywords: 2D h-BN; pulsed laser deposition; room-temperature growth; functional properties; quantum emission

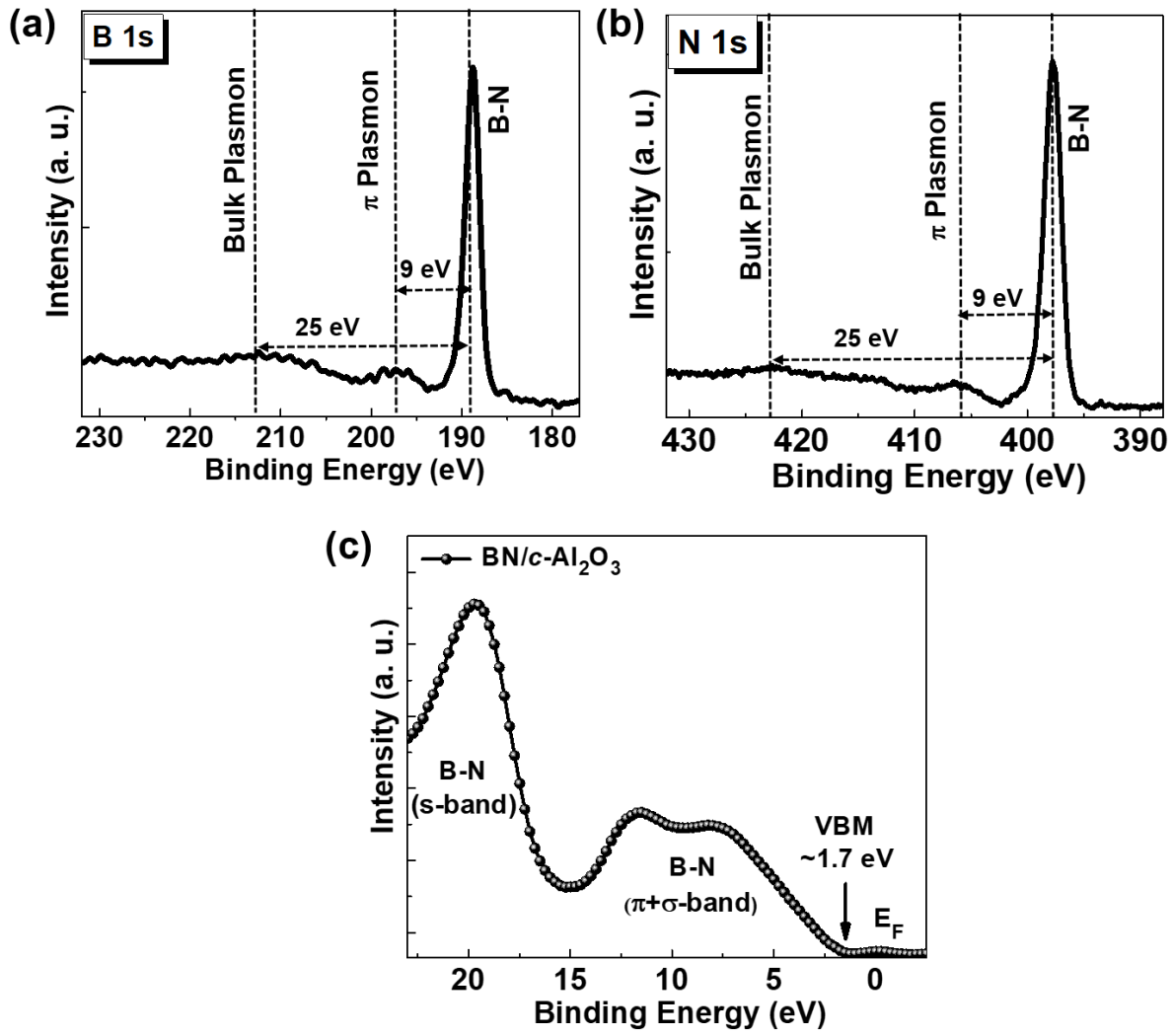

Fig. S1 (a), (b) XPS spectra of a room temperature grown BN film show the characteristic B-N bonding as well as the π-Plasmon and bulk Plasmon peaks of h-BN. (c) Valence band spectra (VBS) shows the characteristics feature of h-BN.

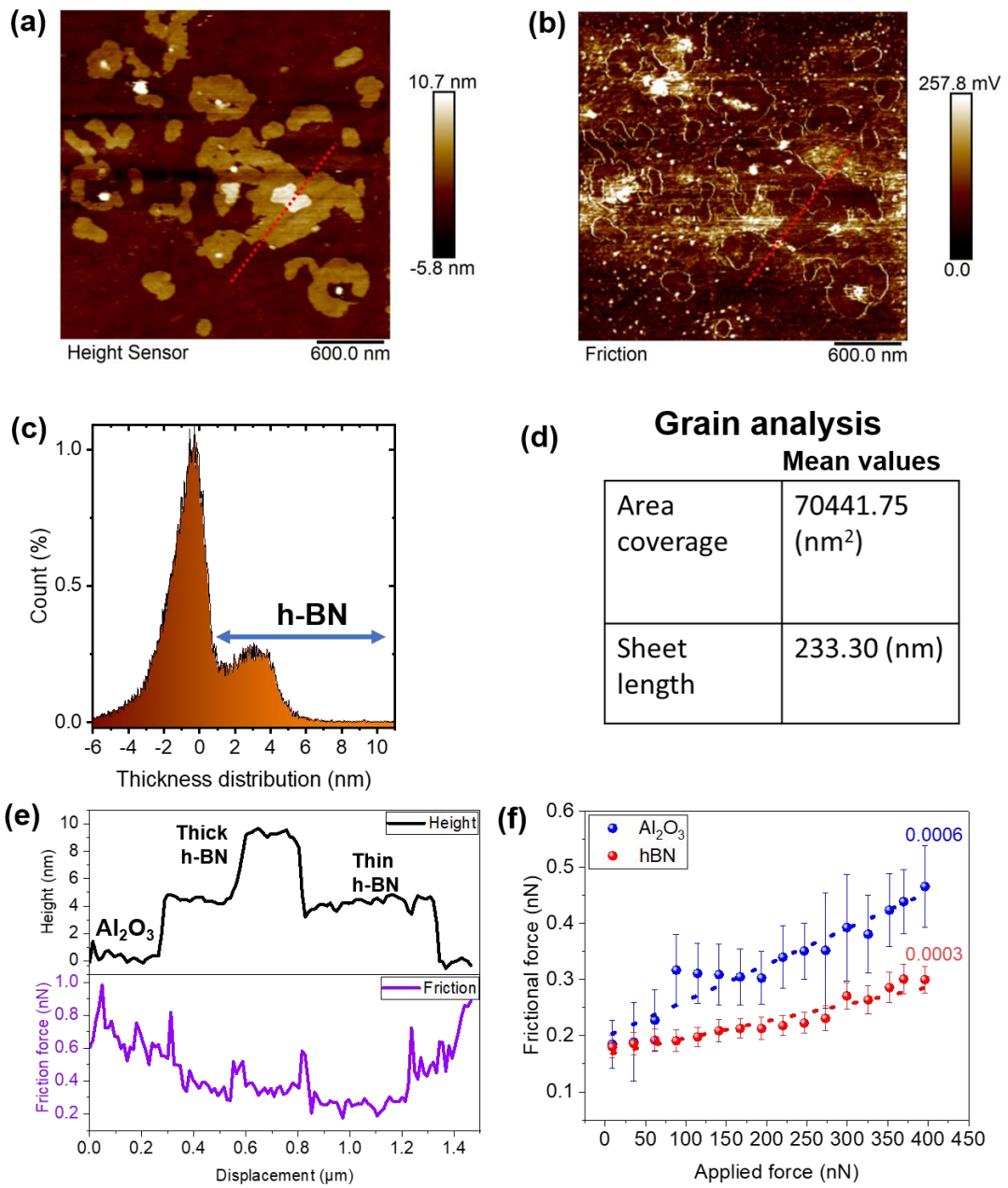

Fig. S2 (a) AFM morphology of h-BN distribution over alumina surface over an area of 3×3 μm^2, and (b) its corresponding frictional force map. (c) The topography-based histogram shows the height distribution of h-BN sheets of different thicknesses varying from 1 to 11 nm, where a majority of the thickness lies in the range of ~3-4 nm. The negative values of the histogram belong to the rough substrate (comprised of roughness, cracks, pit-holes and shallow depression). (d) The grain analysis shows the mean sheet length (assuming round shapes of h-BN sheets) and coverage area. (e) Line profile of the height and the friction at the dotted line in panel (a) and (b). (f) Frictional force of the same region with different loading.

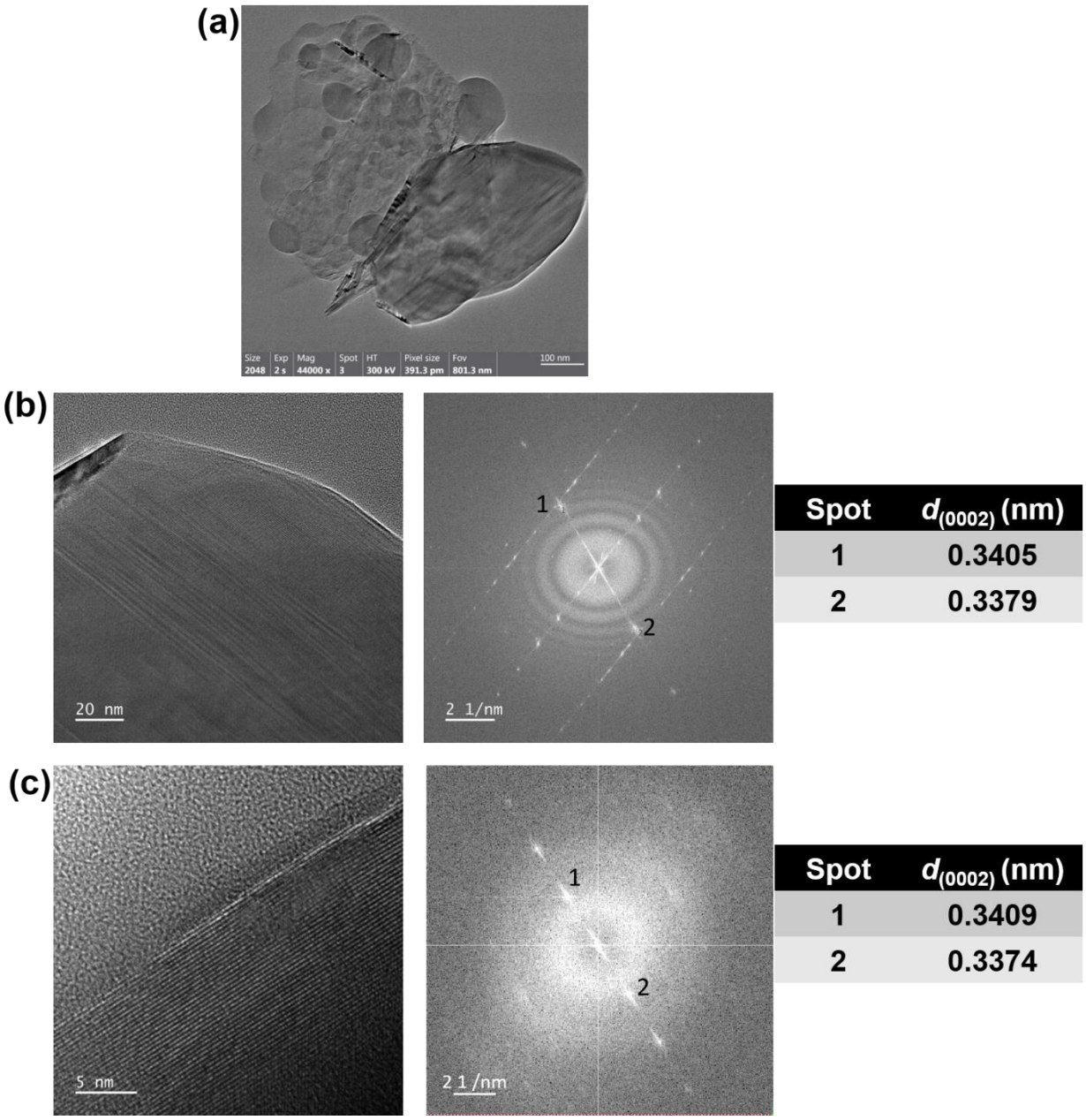

Fig. S3 (a)-(c) Low and high magnification TEM images of deposited flakes on holy Cu-grid at room temperatures. Right panel shows corresponding diffraction patterns and *d* spacing values.

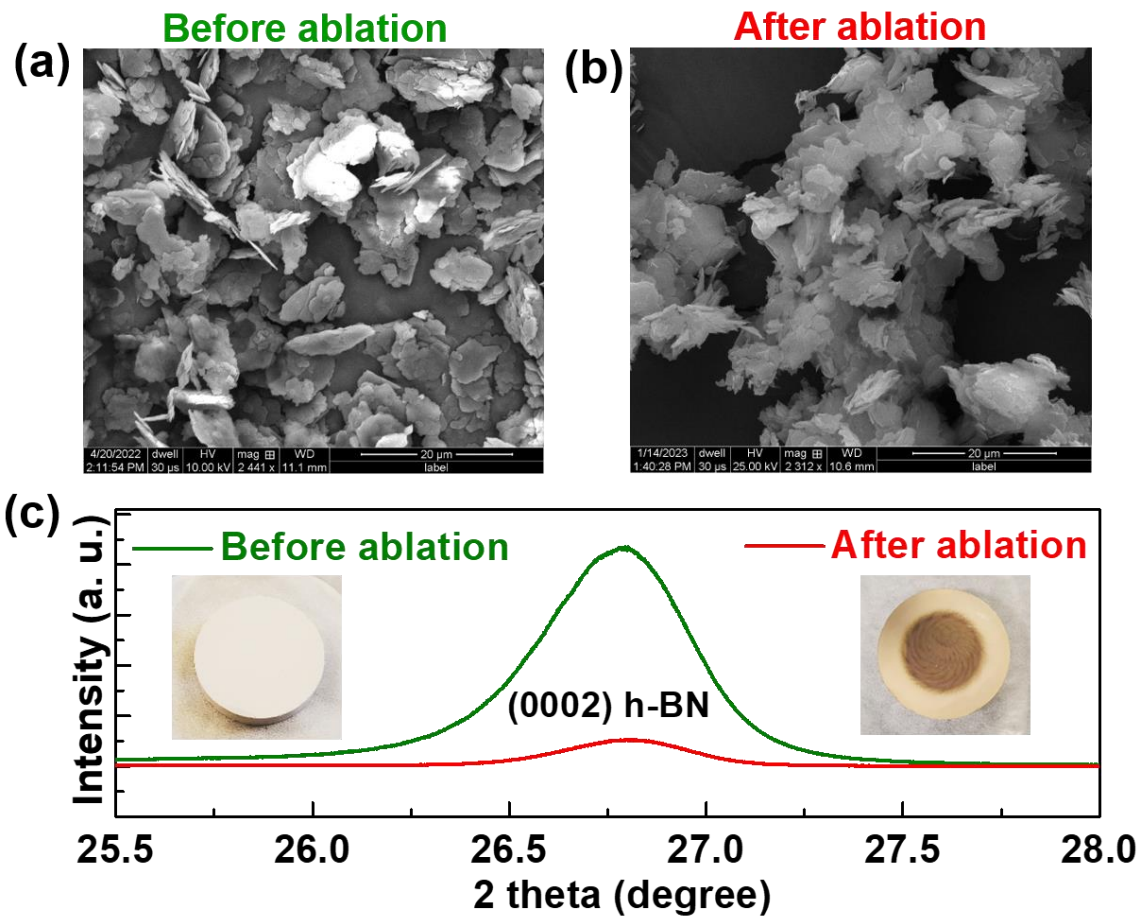

Fig. S4 (a)-(c) FESEM and grazing incident angle XRD (with a low incident angle of 0.1°) of bulk h-BN polycrystalline target (before ablation and after the 10000 shots laser ablation). FESEM were performed by scratching BN powder from the center of the disks and sputtering 10 nm gold on it.

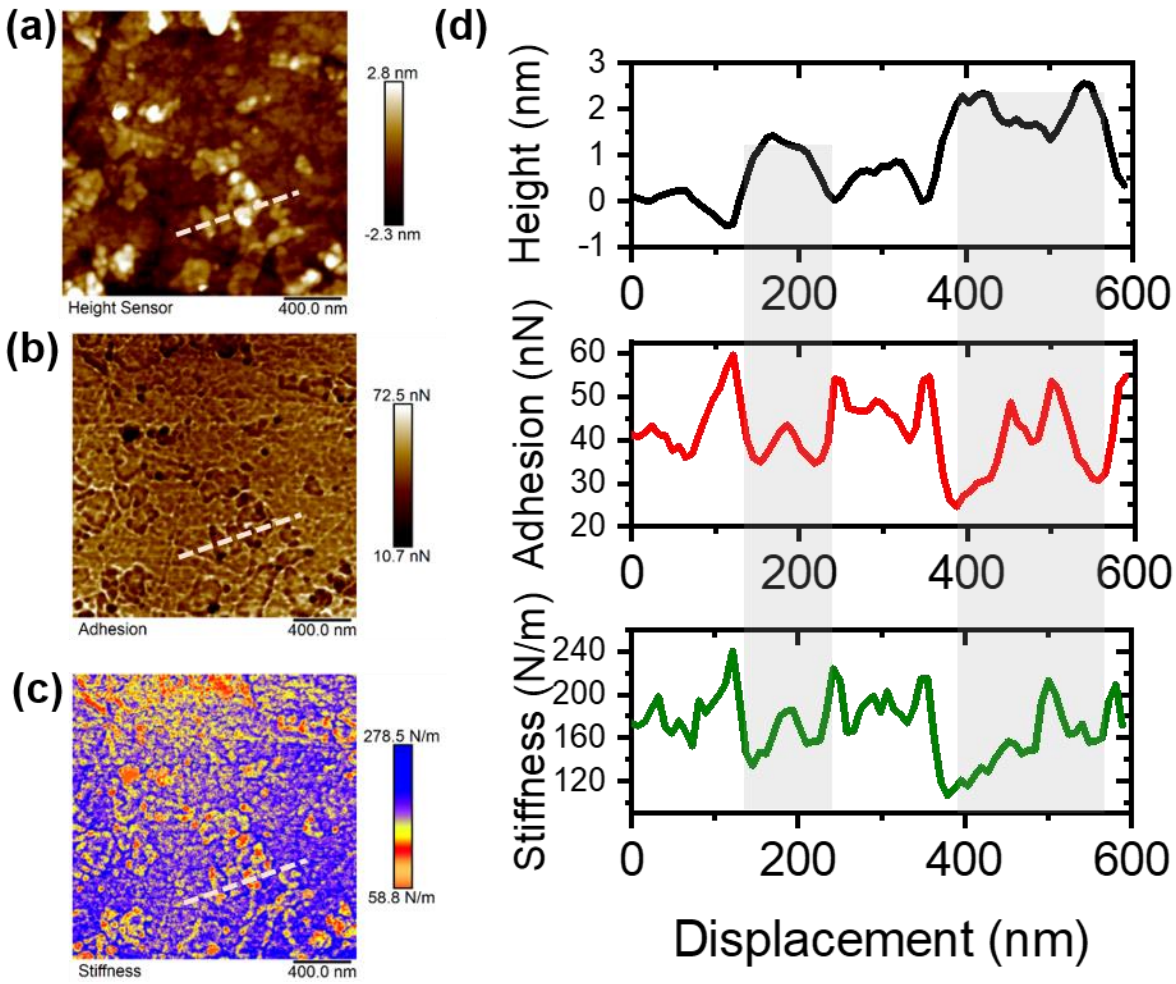

Fig. S5 Thickness dependent measurement of h-BN nanosheets. (a) Topography of h-BN sheets distributed our alumina surface of different thicknesses. (b) Adhesion force (nN) map towards the diamond-like carbon (DLC) tip showing lower adhesion force at thicker h-BN sheets (dark brown region). (c) The stiffness (N/m) map of h-BN sheet over alumina surface. The colour contrast reveals the distribution of h-BN sheet thickness, which is lower at thicker region. (d) line profile corresponding panel (a, b, c) showing the height of the h-BN sheet up to 2.5 nm. The adhesion force values and the stiffness decreases with the thickness (dashed region). The broader tip radii (around 200 nm) of the DLC tip lead to lower resolution in the imaging map.

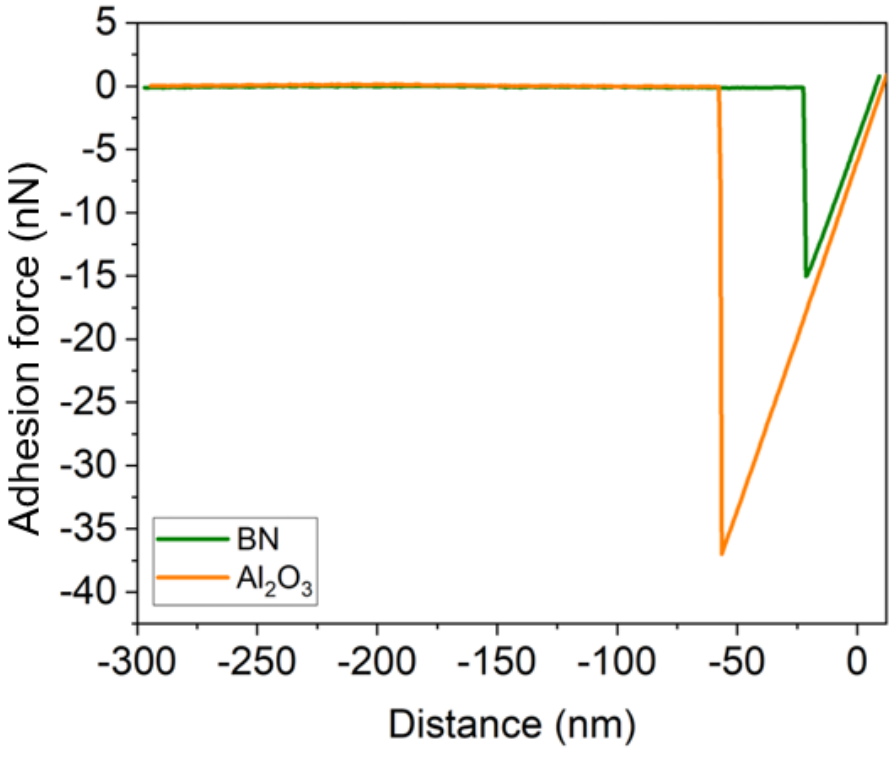

Fig. S6 Force-distance (F-D) spectroscopy carried out by DLC coated probe over BN and alumina surface. The BN is showing the lower pullout force (adhesion force) as compared to alumina.

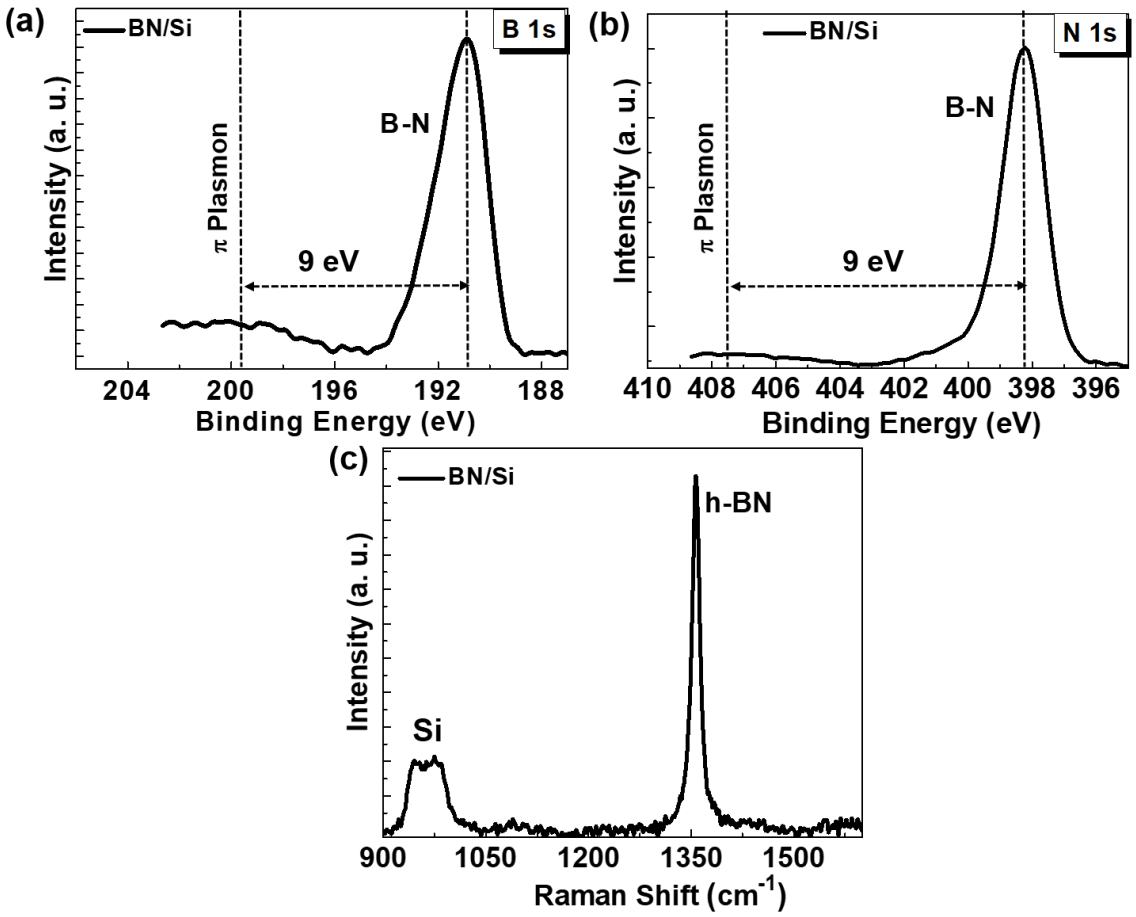

Fig. S7 Characterizations of BN thin films grown on Si (100). (a), (b) XPS elemental B 1s and N 1s core scans confirms the presence of characteristics B-N bonds. (c) Raman spectra shows the peak at ~1359 cm^{-1}, further confirming the growth of h-BN.

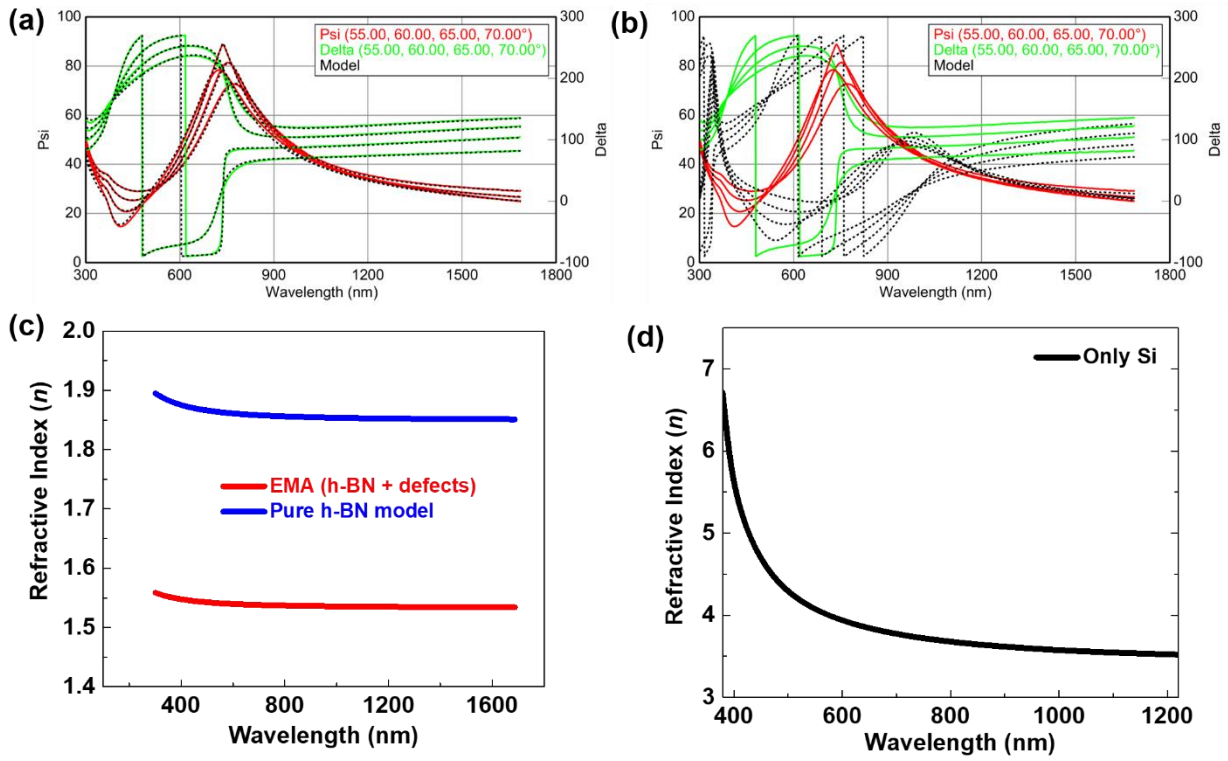

Fig. S8 (a)-(c) Fitting result comparison of different multilayer models used in h-BN film refractive index measurement. (a) Result of a three-layer model consisting of an effective approximation (EMA) layer on the two-layer reference model. (b) Result of a three-layer model consisting of the pure h-BN layer on the two-layer reference model. The h-BN with voids model provide a better fit with a much lower mean square error (MSE) of ~22.525 than for pure h-BN of ~685.652. (c) Obtained RI with two different models. (d) Real part refractive index of Si substrate.